RF Sensing of Personalized Mobility: Accounting for Temporal Variability in Ethogram-Based Classification

Emre Kurtoğlu[a], Sultanus Salehin[a], Moeness G. Amin[b], and Sevgi Z. Gurbuz[a]

[a]Dept. of Electrical & Computer Eng., The University of Alabama, Tuscaloosa, USA
[b]Dept. of Electrical & Computer Eng., Villanova University, Villanova, USA

ABSTRACT

Human activity recognition (HAR) with radar-based technologies has become a popular research area in the past decade. However, the objective of these studies are often to classify human activity for anyone; thus, models are trained using data spanning as broad a swath of people and mobility profiles as possible. In contrast, applications of HAR and gait analysis to remote health monitoring require characterization of the person-specific qualities of a person's activities and gait, which greatly depends on age, health and agility. In fact, the speed or agility with which a person moves can be an important health indicator. In this study, we propose a multi-input multi-task deep learning framework to simultaneously learn a person's activity and agility. In this initial study, we consider three different agility states: slow, nominal, and fast. It is shown that joint learning of agility and activity improves the classification accuracy for both activity and agility recognition tasks. To the best of our knowledge, this study is the first work considering both agility characterization and personalized activity recognition using RF sensing.

Keywords: deep learning, radar, human activity recognition, micro-doppler, spectrograms

1. INTRODUCTION

Human activity recognition (HAR)[1–3] using radar technology has gained significant attention in research, particularly for its applications in security, defense, biomedical fields,[4–8] human-computer interaction[9–11] and indoor monitoring.[12] Existing methodologies in deep learning-based HAR[13] prioritize training models to attain high levels of generalization, ensuring they can effectively recognize activities performed by people who were not encountered during training sessions. In essence, the aim is to learn a generic human mobility profile so that broad activity classes can be recognized for a diverse set of people. This involves training models to encompass a wide range of participant characteristics, such as height, speed, and motion style. The more diverse the dataset that captures various nuances in radar micro-Doppler signatures,[14] the better the model's ability to generalize.

However, it is important to acknowledge that human gait is inherently individualistic and serves as a biometric trait.[15] Every person moves uniquely, influenced by factors like age, health, and mobility. Variations in activities such as walking, kneeling, laying down, or standing up further underscore this uniqueness. For instance, the posture and pace of a healthy teenager vastly differ from those of an elderly individual who is prone to falls. Consequently, applications for remote health monitoring necessitate the characterization and recognition of *person-specific* mobility profiles rather than aiming for generalization across a standardized profile.

Moreover, beyond mere activity recognition, analyzing gait characteristics holds great significance for health monitoring. Recently, there have been an increased number of works considering radar-based gait parameter estimation[16–19] as correlated with health monitoring and fall risk assessment, as well as radar-based implementation of the Timed Up and Go (TUG) test,[20] which is used by physical therapists to evaluate agility and balance. During the TUG test, patients are evaluated not just based on their walking speed but on how agile they can transition from a sit-to-stand position. While traditionally the focus of radar-based HAR has been classification of activities based on fixed duration snapshots of the movement, this approach limits the recognition and

Further author information: (Send correspondence to Sevgi Z. Gurbuz)
Sevgi Z. Gurbuz: E-mail: szgurbuz@ua.edu

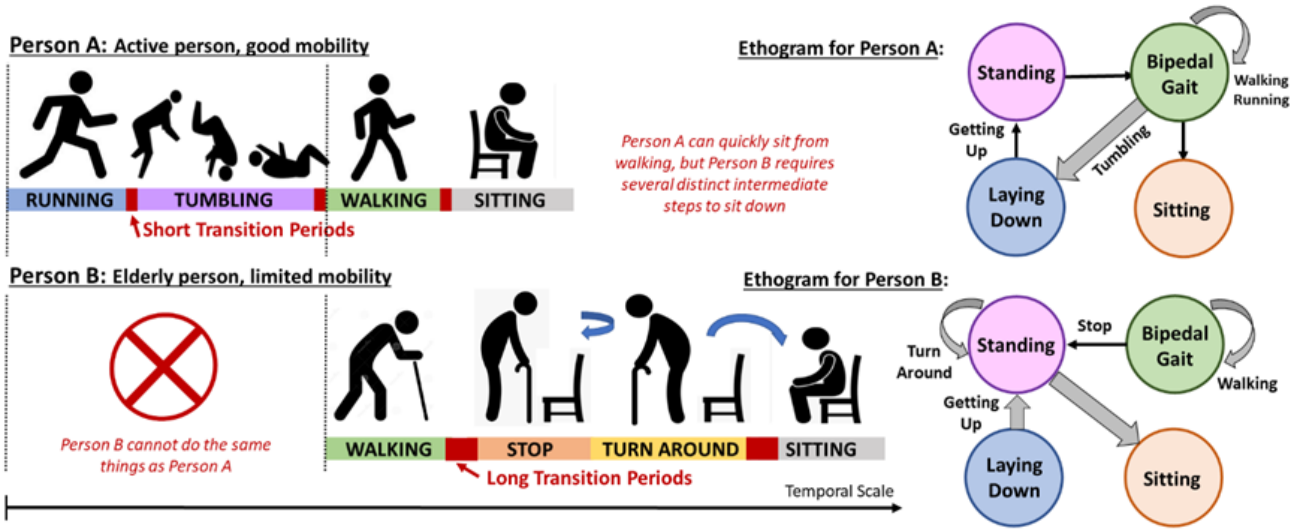

Figure 1: Examples showing person-specific nature of mobility ethograms, which capture both in-state activities and transitional activities.

characterization of activities that are inherently transitionary, such as sit-to-stand, versus persistent, such as walking.

In contrast, the characterization of a person's mobility using ethograms has been recently proposed.[21,22] The term *ethogram*[23,24] used in behavioral psychology is a quantitative description of normal behavior of an animal or a person. When applied to human mobility, an ethogram comprises a state diagram that describes an individual's daily movement patterns in terms of the structure of motion - this is dictated by consideration of not just activity, but the posture with which an activity begins and ends. Each state corresponds to a specific posture, such as ambulatory, standing, sitting or lying down, while activities are categorized as non-transient within a state, like walking, or transient (moving from one state to another) in nature. For instance, falling represents a transient activity wherein an individual instantly transitions from a "standing" state to a "lying down" state. This perspective offers a more nuanced understanding of activities, along with a framework to document the likelihood of particular transitions based on health and mobility, as well as the speed of transition (agility). Together, these elements (i.e., states, in-state and transitional activities, transition probabilities, and agility) constitute the ethogram, providing a comprehensive, person-specific portrayal of one's mobility profile.

An example of how the concept of an ethogram aides in mobility characterization can be seen from Figure 1, which compares the sequential activities and agility of one person who is active with good mobility, and an older adult with limited mobility. While it is possible for an agile person to almost immediately transition from walking to sitting and even do activities such as tumbling, a person of limited mobility may transition over a much longer period of time with intermediate motions. In other words, rather than rapidly transitioning from a walking state to sitting state ("sitting down"), some people may need to first stop, turn around, and then slowly sit down. Real-world data is both sequential and continuous; characterizing the rate of state transitions, i.e. agility, of a person is as important a health indicator as characterizing the actual sequences of motion or extracting gait parameters from intervals of ambulation.

To the best of our knowledge, this study marks the first investigation into utilizing radar technology to jointly characterize and estimate agility alongside transitional activity. Specifically, as a proof of concept, we examine three agility categories denoted by slow, nominal, and fast motion articulations. Our proposed method includes a multi-task deep neural network employing a cumulative loss function consisting of individual losses weighted by adjustable importance factors to simultaneously estimate agility and activity. We demonstrate that our proposed method enhances activity recognition performance while preserving accuracy in agility score estimation, all while requiring significantly fewer trainable parameters and memory resources compared to employing two separate deep neural networks for individual tasks. Furthermore, we explore the incorporation of range information[25,26]

alongside the Doppler information in a multi-input fusion network. To this end, we introduce a multi-input multi-task learning (MIMTL) technique for concurrent recognition of human activity and agility. Our proposed approach enhances activity recognition performance by 6% (from 89.7% to 95.6%) for joint prediction, and 3% (from 95.2% to 98.2%) for multi-task learning approaches, respectively.

The rest of the manuscript is structured as follows: Section 2 outlines the experimental setup, detailing the processes of data collection and pre-processing. In Section 3, various methods for estimating human activity and agility scores are described and compared. Section 4 introduces the proposed MIMTL approach, which jointly estimates activities and agility scores, and provides a comparison with alternative methods. Finally, Section 5 offers concluding remarks, summarizing the key findings of the study.

2. DATA COLLECTION AND EXPERIMENTAL SET UP

2.1 RF Sensor

The frequency-modulated continuous-wave (FMCW) multiple-input multiple-output (MIMO) radar AWR2243BOOST from Texas Instruments is utilized in this work to collect data. The RF sensor operates at at 77 GHz with a 4 GHz bandwidth, enabling range resolution as low as <4 cm. To stream the raw I&Q data, the RF sensor is coupled with a DCA1000EVM data capture board. The beamwidths of the RF antenna are ± 70° in elevation and ± 15° in azimuth.

2.2 Experimental Setup & Data Acquisition

In this study, ten human activities are selected, together with their three distinct agility scores, in order to evaluate the proposed approach's recognition performance. Below is a list of the defined activities and the abbreviations used for them throughout the paper.

- **SITC**: Sitting on a chair
- **STDC**: Standing up from a chair
- **LAYB**: Laying down on an elevated bed
- **GETB**: Getting up from an elevated bed
- **WLKT**: Walking towards radar
- **WLKA**: Walking away from radar
- **PICK**: Picking up an object from the ground with a cane support
- **KNEE**: Kneeling and getting up
- **LAYF**: Laying down on a floor bed
- **GETF**: Getting up from a floor bed

Three distinct speeds (i.e., agility scores) are used for each activity: *slow*, *nominal*, and *fast*. *Slow* activities are those that are typically carried out by participants in a manner that is appropriate for the elderly or those with limited mobility. People who are reading, carrying, or gripping objects may also be preoccupied, which can lead to slow-motion activities. Slow activities were performed by the participants considering these limitations. Activities classified as *Nominal* are conducted at a normal pace and are expressed by a broad age range. Here, each person goes at their own rate while performing the action. Conversely, *Fast* activities are usually associated with healthy, younger people and are usually displayed by those who are rushing. The participants work quickly to complete these exercises. The participants are told to complete the tasks at varying speeds, even though these agility ratings depend on their comprehension of the relative speed at which each task is completed and the radar operator's interpretation of the labels applied to them. A detailed discussion of the activity speed distributions may be found in Section 2.4. The initial of the speed category comes before the activity name to indicate the various speeds for each activity. For example, S_SITC, N_SITC, and F_SITC stand for *slow*, *nominal*, and *fast* performing of SITC, respectively.

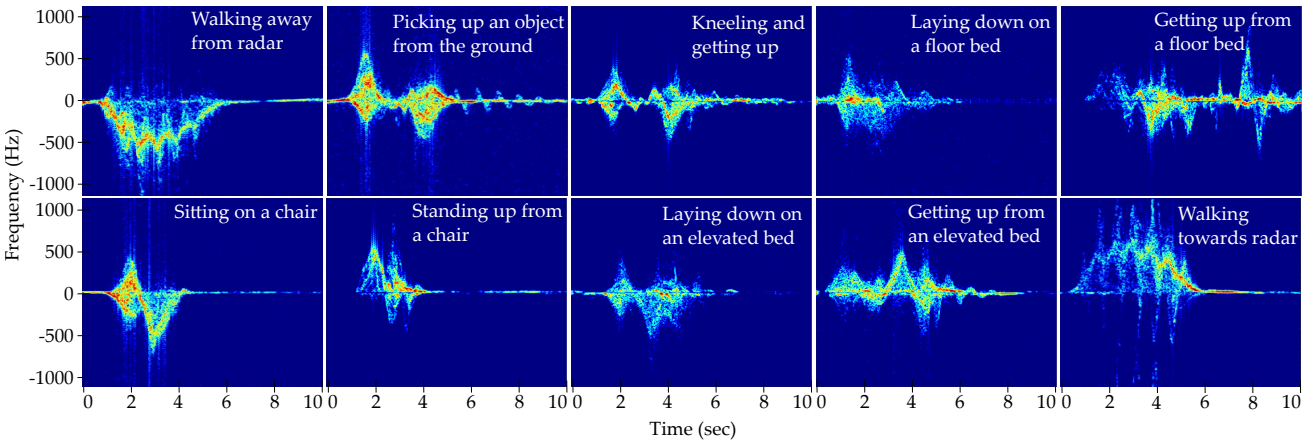

Figure 2: μD spectrograms of different activities.

The radar was positioned about 1 meter above the ground, and transient motions, like walking, had varying distances from the radar than in-place motions, which are carried out in the radar's direct line of sight and at a distance of about 2 meters. Six participants in different ages and genders participated the study, with each recording lasting 10 seconds. In total, 900 samples are collected, which are then split into 70% and 30% portions for training and testing, respectively.

2.3 RF Data Pre-Processing

The transmitted FMCW signal, $S_T(t)$, can be expressed as follows:

$$S_T(t) = \exp(j2\pi f_c t + j\pi\alpha t^2) \tag{1}$$

where f_c represents the carrier frequency and α, the chirp rate, is defined as $\alpha = \frac{B}{T}$, the ratio of bandwidth, B, to sweep time, T. Assuming the transmitted signal reflects back from a set of K targets, the received FMCW signal, $S_R(t)$, can be mathematically represented as time-shifted and frequency-modulated version of the transmitted signal, $S_T(t)$, as follows:

$$S_R(t) = \sum_{i=1}^{K} A_i \exp(j2\pi f_c(t - t_i) + j\pi\alpha(t - t_i)^2) \tag{2}$$

where, A_i is a complex constant related to target's radar cross section, and t_i is the round trip time delay for the i^{th} target.

Radar data cube (RDC), a 3D array, can be created from the raw I&Q data for further processing. In order to obtain the range information, we first apply Fast Fourier Transform (FFT) for each chirp (i.e., pulse) across the analog-to-digital converter (ADC) samples. This process yields the range information over time as a heat map, also known as range profile (RP). The activity time-frequency profiles are produced by windowed Fourier transform over slow-time samples (i.e., chirps), and are referred to as micro-Doppler (μD) signatures.[27] This RF data representation is referred as a spectrogram, and it is calculated as the square modulus of the continuous time input signal's Short-Time Fourier Transform (STFT):

$$S(t, w) = \left| \int_{-\infty}^{\infty} h(t - u)x(u)e^{-jwt}\, du \right|^2 \tag{3}$$

where $h(\cdot)$ is the windowing function, $x(\cdot)$ is the received signal. Figure 2 shows a sample μD spectrogram for each activity.

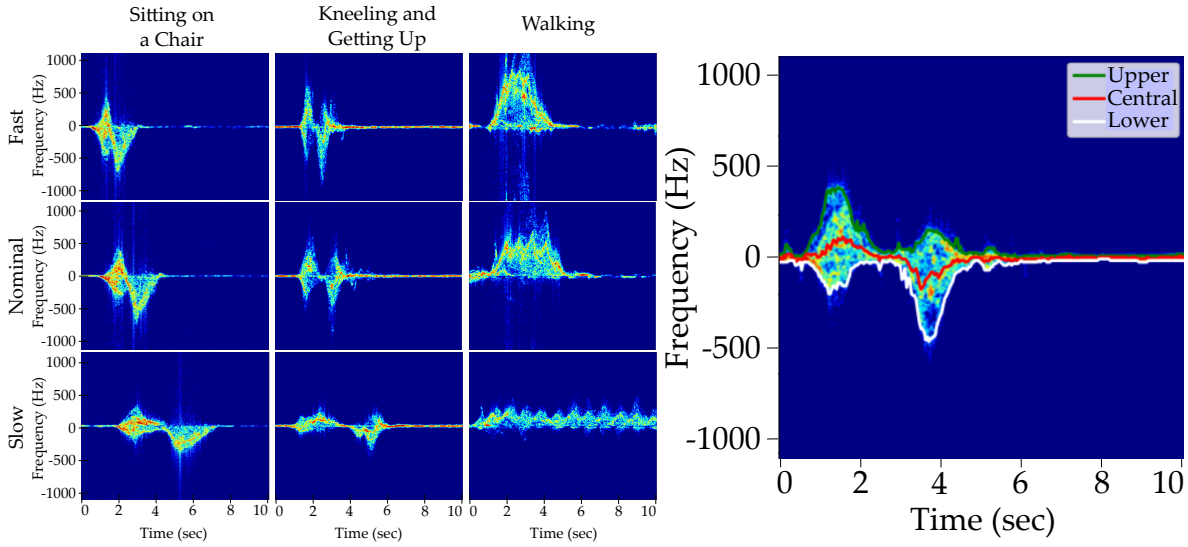

(a) μD spectrograms of activities for varying speeds.

(b) Extraction of upper, central and lower envelopes from μD spectrograms.

Figure 3: Slow, nominal and fast samples for three activities (a), and the result of percentile technique on μD spectrogram.

2.4 Agility Profiles

In the μD spectrogram, varying activity speeds might manifest as compression or expansion behavior in time and frequency. While *slow* movements cause compressing in frequency and expansion in time axis, *fast* motions demonstrate the opposite with expansion in time and compression in frequency. Three activities—SITC, KNEE, and WLKT are used to demonstrate this phenomenon in Figure 3a. It can be seen that as the activities are completed more slowly (from top to bottom), the frequency band narrows down and the total activity time increases. Such variations in activity level can be an indicator of mobility limitations, abnormalities or health problems. Therefore, in health applications, it is crucial to accurately identify agility score of the person.

In order to detect minimum and maximum velocities occurred during an activity, we employ the percentile technique[28] to extract the upper, central, and lower envelopes of the μD signatures. Figure 3b illustrates the extracted envelopes. The maximum velocity distribution of the *slow*, *nominal*, and *fast* samples is shown in Figure 4. It can be observed that *slow* samples have much lower mean peak velocity of 2.19 m/s when compared to the *fast* samples which have an average maximum velocity of 3.45 m/s. Majority of the *Nominal* samples, on the other hand, have peak velocity in-between the two extreme cases with the mean peak velocity of 2.84 m/s. It should be mentioned that all of the classes are included in these distributions, and that some activities inherently have lower radial motion than others, which may cause the distributions to overlap in certain velocity intervals. For example, F_LAYB and S_WLKT may have comparable radial speeds. Therefore, we can expect certain amount of overlap between the distributions given the nature of the activities.

3. ACTIVITY AND AGILITY ESTIMATION

In this work, we evaluated four DL-based methods for recognizing activity and agility scores. They can be listed as: recognizing activity only, recognizing agility only, estimating activity and agility jointly, and estimating activity and agility simultaneously in a multi-task fashion. An identical backbone network is used for feature extraction so that a fair comparison across various methods is ensured. The VGG-16 network was chosen because of its effectiveness on different RF datasets[29].[30]

The architectures of the two distinct networks, activity-only and agility-only are the same, with the exception of the quantity of neurons in the output classification layer. The joint activity and agility prediction network creates 30 (10×3) neurons at the output layer by combining activity and agility recognition into a single job

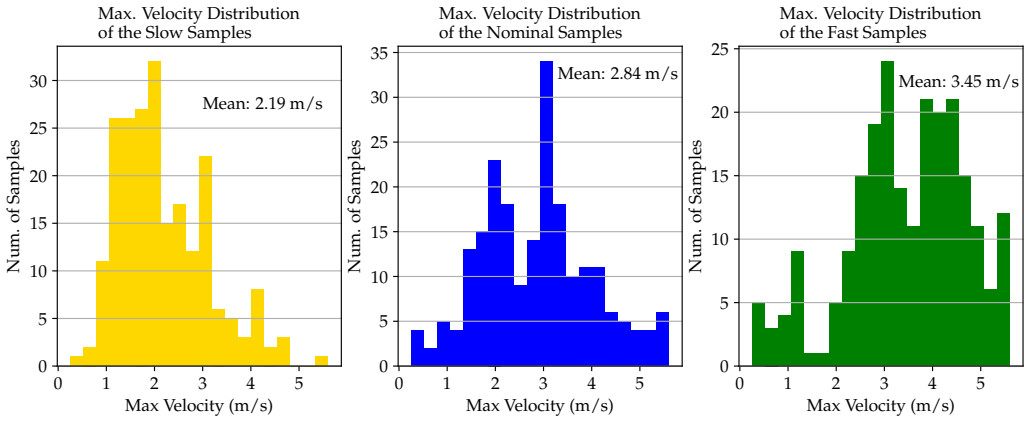

Figure 4: Maximum velocity distributions of different agility scores.

Table 1: Performance comparison of different activity and agility score recognition approaches.

Recognition Method	**Number of Output Classes**	**Acc. (%) Activity**	**Acc. (%) Agility**
Activity Only	10	95.9	-
Agility Only	3	-	89.7
Joint Act. & Ag.	30	89.7	91.9
Multi-task Act. & Ag.	10 & 3	95.2	90.8

that estimates activity and its agility score. In the multi-task learning approach, on the other hand, the network has two distinct output layers, having 10 and 3 neurons for activity and agility prediction. The combined loss, $\mathcal{L}_{\text{total}}$, for the two tasks can be written as:

$$\mathcal{L}_{\text{total}} = \lambda \mathcal{L}_{\text{act}} + \gamma \mathcal{L}_{\text{ag}} \tag{4}$$

where the weights of two losses are λ and γ, and $\mathcal{L}_{\text{act}}$ and $\mathcal{L}_{\text{ag}}$ are the categorical cross-entropy losses for activity and agility recognition tasks. To avoid any bias towards a particular task, both λ and γ are set to 1.

The classification results for the four previously described methods are shown in Table 1. Although the activity-only and the agility-only networks achieve high classification accuracy rates of 95.9% and 89.7%, respectively, they are primarily designed for single task. Furthermore, they need different networks, which doubles the amount of memory and processing power needed. Conversely, the joint estimate network integrates the two tasks into a single network with 30 neurons in a broader output layer. It permits the two tasks to be optimized simultaneously. Although this network's total testing accuracy for 30 classes is 82.3%, separate metrics of 89.7% and 91.9% can be derived by combining agility and activities scores for a specific task. The pooling operation for the activity recognition evaluation from 30-class to 10-class is depicted in Figure 5a. The predictions of the agility score within the same activity category are shown by the red squares, which can be combined to ignore any inaccuracies resulting from the agility estimation. On the other hand, Figure 5b illustrates the pooling operation for agility recognition which changes number of prediction outputs from 30-class to 3-class. The predictions of the activity within the same agility category are shown by the red squares, which can be combined to ignore the activity prediction errors. The regions where *slow* and *fast* actions are confused with one another is indicated by the blue squares that are off-diagonal. Given that all the cells are zero, it is evident that there is no confusion. Note that the numbers in the confusion matrices indicate the number of samples, not the percentages.

While the accuracy of agility in joint prediction approach is higher than the accuracy of the agility-only network, the accuracy of activities is much lower than the activity-only network. This suggests that agility differentiation is given greater weight in the network than activity differentiation. In this approach, we are unable to prioritize any one task, which is a result of the network having a single output for measuring both

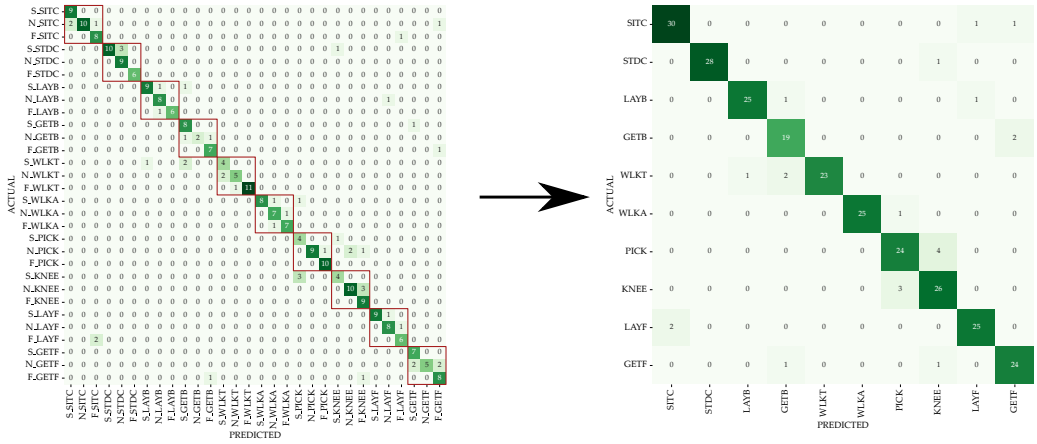

(a) Confusion matrix of 30-class activity and agility score estimation (left) and merging of different agility scores of the same activity into the same cell (right).

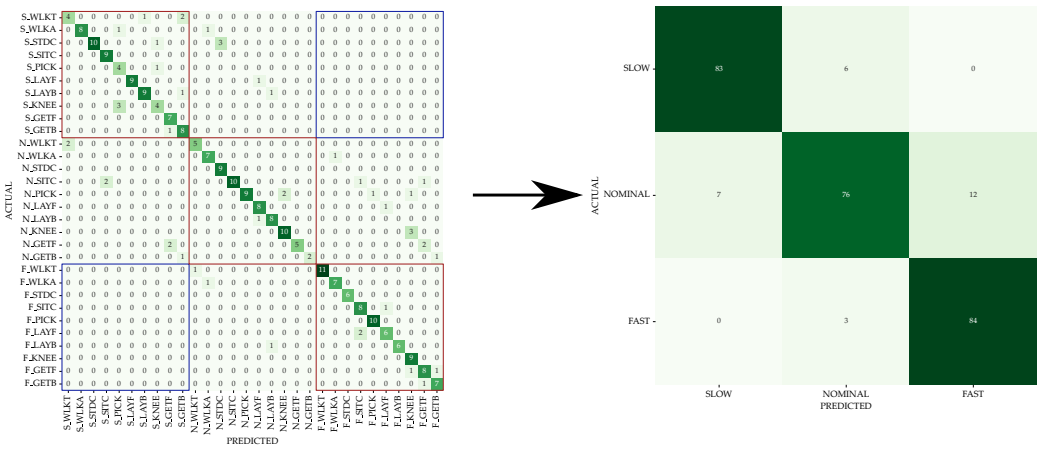

(b) Rearranged confusion matrix of 30-class activity and agility score estimation (left) and merging of different classes with the same agility score into the same cell (right).

Figure 5: Confusion matrices of joint activity and agility score estimation.

activity and agility. This necessitates a less constrained strategy: multi-task learning. It is possible to assign an arbitrary relevance coefficient to each objective by having distinct outputs for each task. Accuracies of 95.2% and 90.8% are obtained by the multi-task technique for the activity and agility recognition tasks, respectively. Although the agility performance is in between the joint and the agility-only approaches with minor differences, the activity performance is significantly better than the joint case and nearly as good as the activity-only network.

4. MULTI-INPUT MULTI-TASK LEARNING NETWORK

μD spectrograms are an effective tool for displaying the kinematics of the body over time, but they do not reveal the precise locations of the body parts. In this section, we assess how well RPs deliver the range information to the network. The same VGG-16 backbone network is used for one-to-one comparisons. But because the network receives both μD spectrograms and RPs at the same time, two parallel VGG-16 branches are built for feature extraction, which are then followed by task-specific fully connected layers. The concatenation layer aggregates the latent spaces of the two inputs after the multi-layer perceptron (MLP) layers. Lastly, two output layers are added for the classification of agility and activity. Figure 6 shows the MIMTL network's overall architecture.

The performance of the MIMTL network is benchmarked with the multi-input joint activity and agility estimation network, which shares the same model architecture but only has one output layer with thirty neurons for classification as opposed to having two output layers with ten and three neurons.

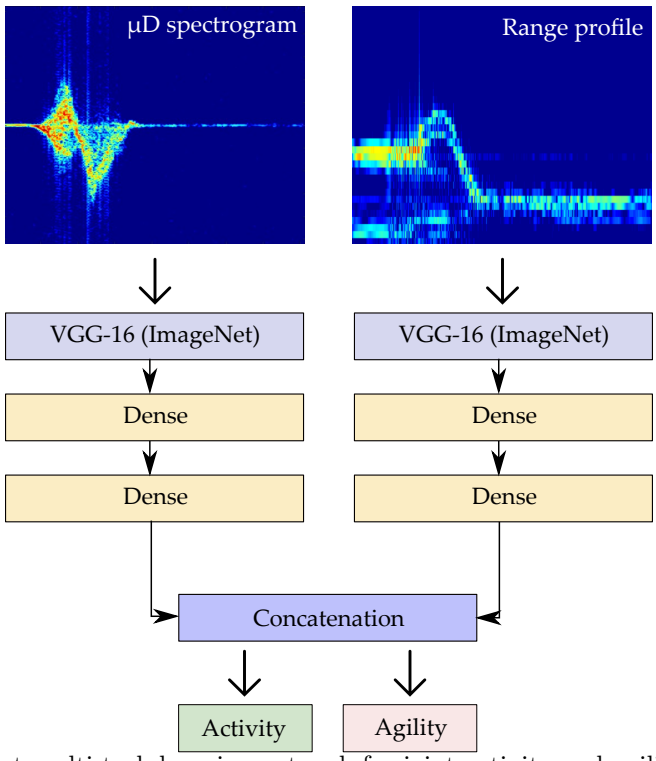

Figure 6: Multi-input multi-task learning network for joint activity and agility score prediction.

The classification results for the four alternative approaches (i.e., μD-only joint estimate, μD-only multi-tasking, multi-input joint estimation, and MIMTL method) for activity and agility recognition are shown in Figure 7. When the network is constructed as multi-task instead of joint estimating activity and agility score for single and multi-input situations, it is noticed that the accuracy of activity identification is consistently improved from 89.7% to 95.2% and from 95.6% to 98.2% for single and multi-input cases, respectively. Additionally, the recognition ability of activities for both joint (89.7% to 95.6%) and multi-task (95.2% to 98.2%) approaches are enhanced by the inclusion of range information. For the agility score recognition task, there is only a slight decrease in performance (from 91.9% to 90.8%) and a subtle rise (from 88.2% to 90%) for single and multi-input networks.

5. CONCLUSION

This paper presented the first work on joint estimation of human activities of daily living and the activity agility score. The initial study combining the activity agility score and human activities of daily living estimation is provided in this paper. We investigate the inclusion of a person's ethogram information through agility score into the activity estimation. This reflects the idea of having a prior knowledge about a person's mobility profile while predicting the current activity, which provides additional information to the network and serves as a regularizer in the training stage. For the simultaneous classification of both tasks, we evaluated various strategies. It is inferred that the best performance for activity recognition while preserving the accuracy of the agility score estimation is attained when both tasks (activity recognition and agility characterization) are optimized in different output layers using a joint total loss function. By modifying the individual loss weight coefficients, the importance of each objective can be adjusted.

In addition, it was demonstrated that adding range data alongside Doppler data in a multi-input manner improves the accuracy of activity detection while preserving the agility score recognition performance. This suggests that human activities and a person's present level of agility can be recognized using the MIMTL technique via RF sensing. Abrupt or gradual changes in the agility score can be signs of certain gait disorders or healing processes, depending on the direction of the change. Although our analysis only examined three labels

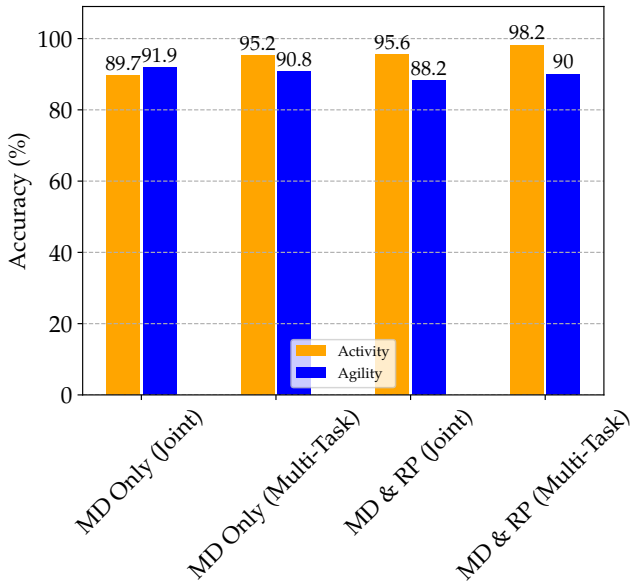

Figure 7: Comparison of joint and multi-task estimation results for single and multi-input networks.

for agility scores, it lays the groundwork for future generalization and sophisticated joint activity recognition and agility state characterization approaches.

ACKNOWLEDGMENTS

The National Science Foundation (NSF) provided funding for this work under awards #223503 and #2238653. Research involving human subjects was carried out in accordance with UA Institutional Review Board (IRB) Protocols #18-06-1271 and #23-04-6553.

REFERENCES

[1] Gurbuz, S. Z. and Amin, M. G., "Radar-based human-motion recognition with deep learning: Promising applications for indoor monitoring," *IEEE Signal Processing Magazine* **36**(4), 16–28 (2019).

[2] Kim, Y. and Moon, T., "Human detection and activity classification based on micro-doppler signatures using deep convolutional neural networks," *IEEE Geosci.Rem. Sens. Lett.* **13**(1), 8–12 (2016).

[3] Erol, B., Gurbuz, S. Z., and Amin, M. G., "Motion classification using kinematically sifted acgan-synthesized radar micro-doppler signatures," *IEEE Transactions on Aerospace and Electronic Systems* **56**(4), 3197–3213 (2020).

[4] Li, C., Cummings, J., Lam, J., Graves, E., and Wu, W., "Radar remote monitoring of vital signs," *IEEE Microwave Magazine* **10**(1), 47–56 (2009).

[5] Shah, S. A. and Fioranelli, F., "Rf sensing technologies for assisted daily living in healthcare: A comprehensive review," *IEEE Aerospace and Electronic Systems Magazine* **34**(11), 26–44 (2019).

[6] Jokanović, B. and Amin, M., "Fall detection using deep learning in range-doppler radars," *IEEE Transactions on Aerospace and Electronic Systems* **54**(1), 180–189 (2018).

[7] Amin, M. G., Zhang, Y. D., Ahmad, F., and Ho, K. D., "Radar signal processing for elderly fall detection: The future for in-home monitoring," *IEEE Signal Processing Magazine* **33**(2), 71–80 (2016).

[8] Seyfioğlu, M. S., Özbayoğlu, A. M., and Gürbüz, S. Z., "Deep convolutional autoencoder for radar-based classification of similar aided and unaided human activities," *IEEE Transactions on Aerospace and Electronic Systems* **54**(4), 1709–1723 (2018).

[9] Lien, J., Gillian, N., Karagozler, M. E., Amihood, P., Schwesig, C., Olson, E., Raja, H., and Poupyrev, I., "Soli: Ubiquitous gesture sensing with millimeter wave radar," *ACM Trans. Graph.* **35**(4) (2016).

[10] Gurbuz, S. Z., Gurbuz, A. C., Malaia, E. A., Griffin, D. J., Crawford, C. S., Rahman, M. M., Kurtoglu, E., Aksu, R., Macks, T., and Mdrafi, R., "American sign language recognition using rf sensing," *IEEE Sensors Journal* **21**(3), 3763–3775 (2021).

[11] Kurtoğlu, E., Gurbuz, A. C., Malaia, E. A., Griffin, D., Crawford, C., and Gurbuz, S. Z., "Asl trigger recognition in mixed activity/signing sequences for rf sensor-based user interfaces," *IEEE Transactions on Human-Machine Systems* **52**(4), 699–712 (2022).

[12] Amin, M., [*Radar for Indoor Monitoring: Detection, Classification, and Assessment*], CRC Press (2018).

[13] Gurbuz, S. Z., ed., [*Deep Neural Network Design for Radar Applications*], IET, London (2020).

[14] Gurbuz, S. Z. and Amin, M. G., [*Micro-Doppler Radar and its Applications*], ch. Deep neural networks for radar micro-Doppler signature classification, 103–135, IET, London, UK (2020).

[15] Isaac, E., Elias, S., Rajagopalan, S., and Easwarakumar, K., "Trait of gait: A survey on gait biometrics," (03 2019).

[16] Wang, F., Skubic, M., Rantz, M., and Cuddihy, P. E., "Quantitative gait measurement with pulse-doppler radar for passive in-home gait assessment," *IEEE Transactions on Biomedical Engineering* **61**(9), 2434–2443 (2014).

[17] Seifert, A.-K., Grimmer, M., and Zoubir, A. M., "Doppler radar for the extraction of biomechanical parameters in gait analysis," *IEEE Journal of Biomedical and Health Informatics* **25**(2), 547–558 (2021).

[18] Saho, K., Shioiri, K., Kudo, S., and Fujimoto, M., "Estimation of gait parameters from trunk movement measured by doppler radar," *IEEE Journal of Electromagnetics, RF and Microwaves in Medicine and Biology* **6**(4), 461–469 (2022).

[19] Gurbuz, S. Z., Kurtoglu, E., Rahman, M. M., and Martelli, D., "Gait variability analysis using continuous rf data streams of human activity," *Smart Health* **26**, 100334 (2022).

[20] Soubra, R., Mourad-Chehade, F., and Chkeir, A., "Automation of the timed up and go test using a doppler radar system for gait and balance analysis in elderly people," *Journal of Healthcare Engineering* **2023** (06 2023).

[21] Amin, M. G., "Micro-doppler classification of activities of daily living incorporating human ethogram," in [*SPIE DCS Symp.*], (2020).

[22] Amin, M. G. and Guendel, R. G., "Radar classifications of consecutive and contiguous human gross-motor activities," *IET Radar, Sonar & Navigation* **14**(9), 1417–1429 (2020).

[23] Jesness, B., "A human ethogram: Its scientific acceptability and importance (now new, because new technology allows investigation of the hypotheses) (an early must read)," (02 1985).

[24] Jones, L. K., Jennings, B. M., Higgins, M. K., and de Waal, F. B. M., "Ethological observations of social behavior in the operating room," *Proceedings of the National Academy of Sciences* **115**(29), 7575–7580 (2018).

[25] Erol, B., Amin, M., and Boashash, B., "Range-doppler radar sensor fusion for fall detection," 0819–0824 (05 2017).

[26] Erol, B. and Amin, M., "Fall motion detection using combined range and doppler features," 2075–2080 (08 2016).

[27] Chen, V., [*The Micro-Doppler Effect in Radar, Second Edition*], Artech House (2019).

[28] Dorp, P. V. and Groen, F. C. A., "Feature-based human motion parameter estimation with radar," *IET Radar, Sonar Navigation* **2**(2), 135–145 (2008).

[29] Simonyan, K. and Zisserman, A., "Very deep convolutional networks for large-scale image recognition," *arXiv preprint arXiv:1409.1556* (2014).

[30] Deng, J., Dong, W., Socher, R., Li, L.-J., Li, K., and Fei-Fei, L., "Imagenet: A large-scale hierarchical image database," in [*2009 IEEE Conference on Computer Vision and Pattern Recognition*], 248–255 (2009).